KTH Alfvén Laboratory

Workshop on Active control of MHD Stability, Princeton, NJ, 6-8 Nov., 2006

RWM control in T2R

Per Brunsell

P. R. Brunsell[1], J. R. Drake[1], D. Yadikin[1], D. Gregoratto[2], R. Paccagnella[2], Y. Q. Liu[3], T. Bolzonella[2], M. Cecconello[1], M. Kuldkepp[4], G. Manduchi[2], G. Marchiori[2], L. Marrelli[2], P. Martin[2], S. Menmuir[4], S. Ortolani[2], E. Rachlew[4], G. Spizzo[2], P. Zanca[2]

1) Alfvén Lab., Association EURATOM-VR, Royal Inst. of Technology, Stockholm, Sweden

2) Consorzio RFX, Associazione EURATOM-ENEA sulla fusione, Padova, Italy

3) Dept. of Appl. Mechanics, Association EURATOM-VR, Chalmers Univ. of Technology, Gothenburg, Sweden

4) Dept. of Physics, Association EURATOM-VR, Royal Inst. of Technology, Stockholm, Sweden

Motivation for present work

The T2R reversed-field pinch is well suited for basic studies of RWM control. Emphasis is on **comparison of experiment with theory**:

- Unstable modes are driven by the equilibrium current density gradient and therefore easily parameterized in both experiment and theory, and **modes can be studied at low current.**
- Modes are **helical harmonics** characterized by poloidal and toroidal mode numbers (m=1, n) with **facilitates the use of a toroidal array of saddle coils** as sensors and active coils.
- Modes are non-resonant (there is no surface where q=-m/n inside the plasma) and their **stability is not affected by sub-Alfvénic plasma rotation.**
- Circular cross-section and large aspect ratio makes **comparison with cylindrical linear MHD model very effective.**

Outline of talk

1. Active MHD mode control system on T2R
2. Comparison of cylindrical MHD model with T2R data
3. Intelligent shell fb with 4x32 coils (full surface cover)
4. Toroidal side band coupling with 4x16 coil feedback
5. Poloidal side band coupling with 2x32 coil feedback
6. Test of simplified fake rotating shell feedback
7. Mode control feedback with complex fb gain

Active MHD mode control system on T2R

EXTRAP T2R reversed field pinch

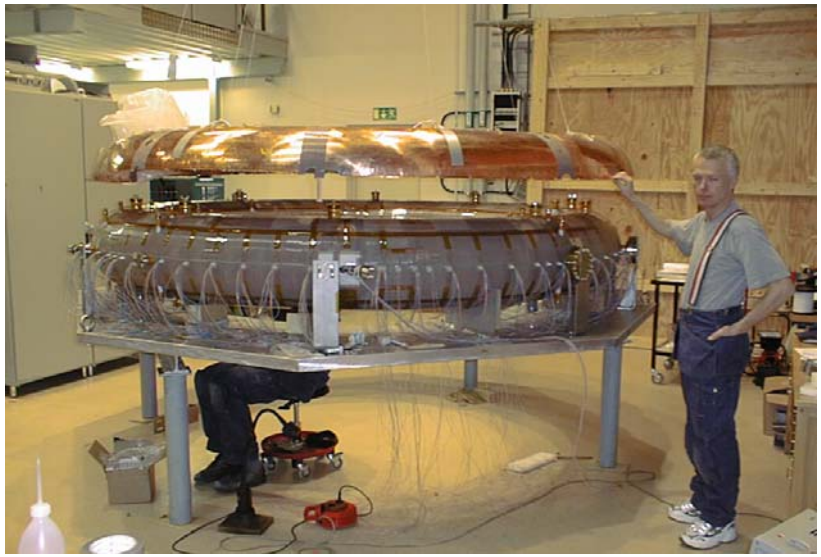

EXTRAP T2R new vessel and shell during assembly at Alfvén Laboratory, KTH, Stockholm

Machine parameters:

- major radius R_0=1.24 m
- plasma minor radius a=18 cm
- shell norm minor radius r/a = 1.08
- shell time constant τ_{ver}=6 ms
- plasma current I_p=80 kA
- electron temperature T_e=250 eV
- pulse length τ_{pulse}< 60 ms

Pulse lengths $\tau_{pulse} >> \tau_{ver}$ allow studies of RWM stability and methods for active control of RWMs

T2R device (with OHTE iron-core, pol. coils, and platform)

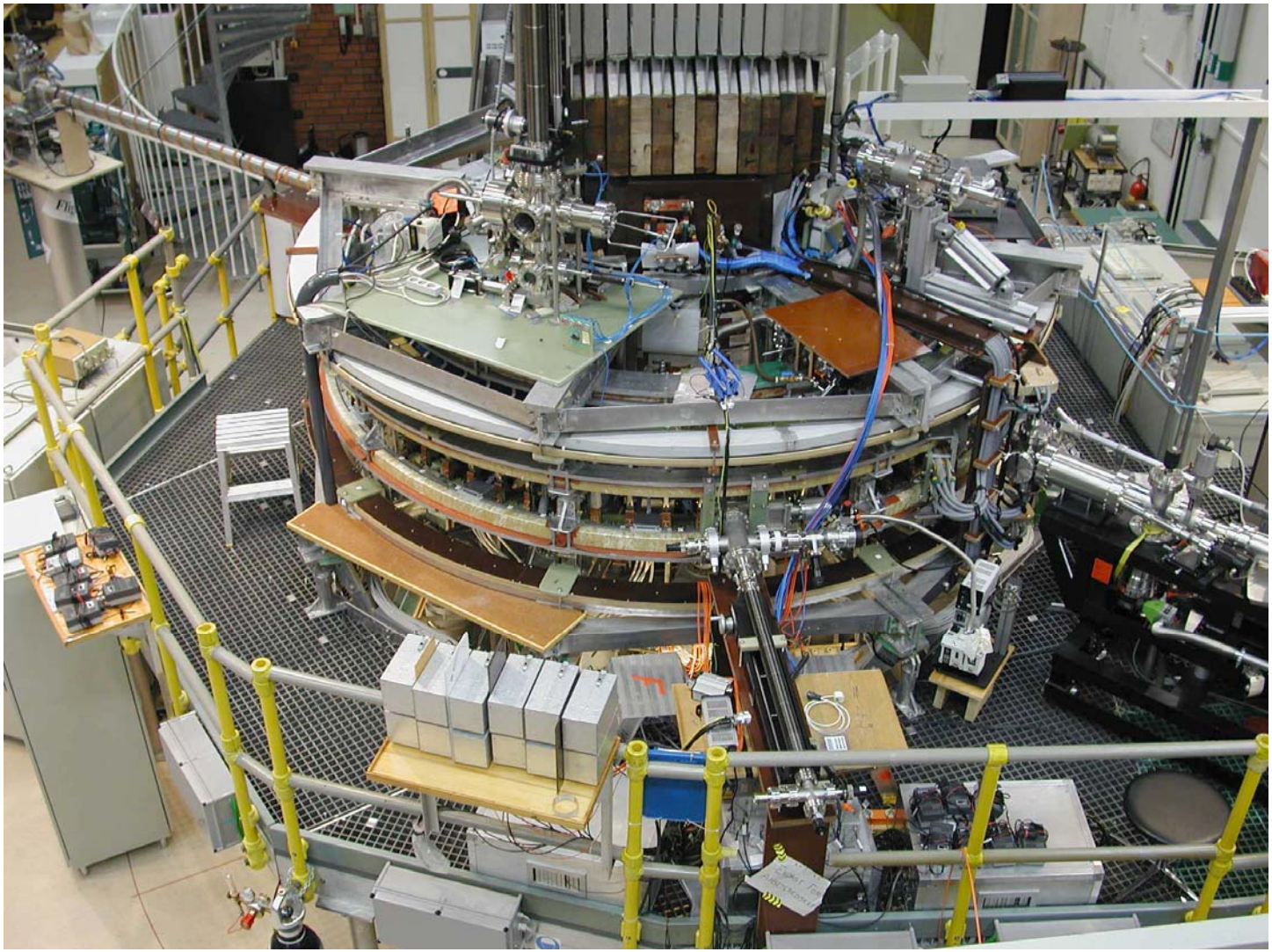

Cross-section view of T2R vessel, copper shell, sensors and active saddle coils

Stainless vacuum vessel bellows and Mo limiters

Copper shell, two layers, each 0.5 mm thick

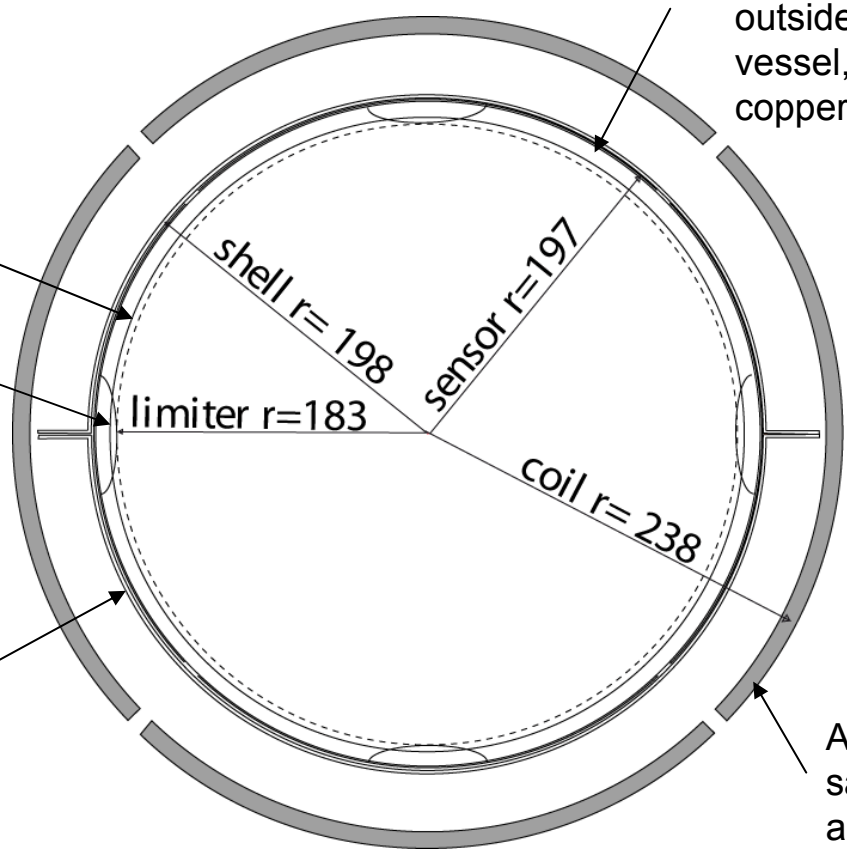

Sensor loops are mounted on outside surface of vessel, inside copper shell

Active saddle coils are outside shell

radii in mm

T2R saddle coil arrays

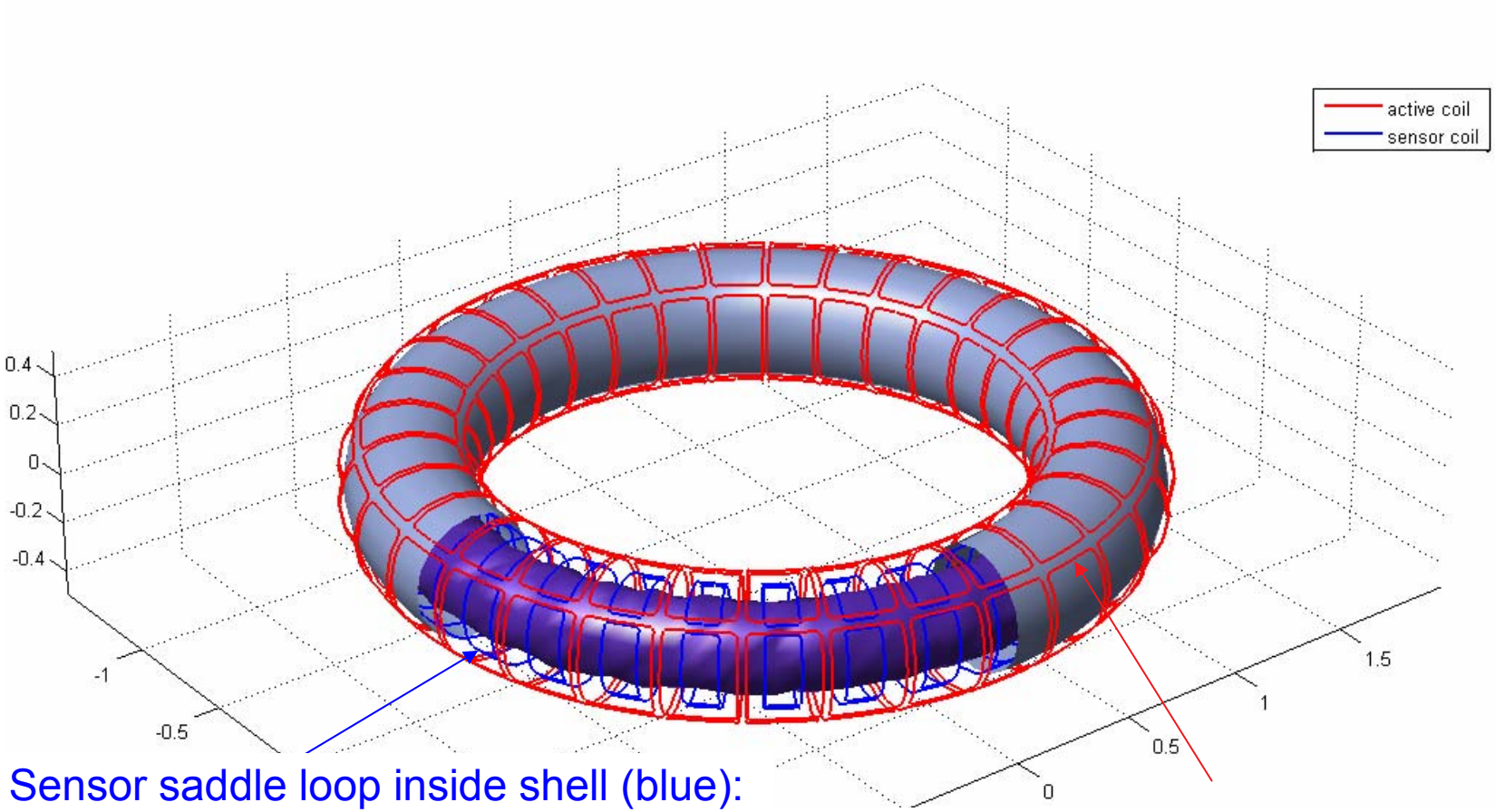

Sensor saddle loop inside shell (blue):

- norm. radius: $r_c/a=1.08$
- coil span: 90^o poloidal, 5.6^o toroidal
- 50 % surface cover

Active saddle coil outside shell (red):

- norm. radius: $r_c/a=1.3$
- coil span: 90^o poloidal, 11.2^o toroidal
- 100 % surface cover

T2R MHD Control System

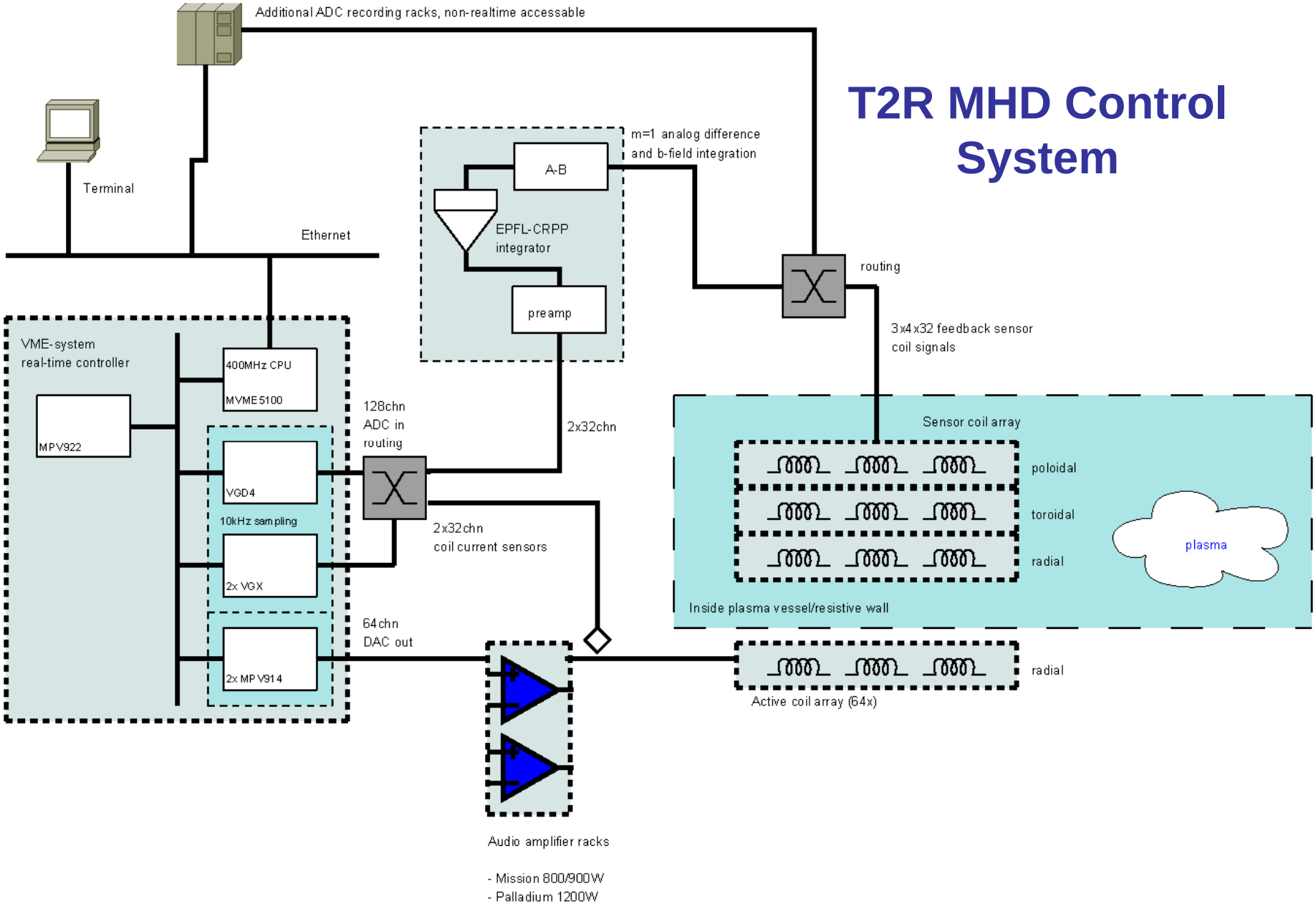

Comparison of cylindrical MHD model with T2R data

Cylindrical MHD model - saddle coil vacuum field spectrum

Vacuum radial field harmonic at wall $b_{m,n}$ from coil current harmonic $I_{m,n}$:

Long wall time constant: $\tau_w = \mu_0 \sigma r_w \delta_w$

Mode wall time: $\tau_{m,n}$

Coil field mode amplitude: $M_{m,n}=b_{m,n} / I_{m,n}$

$$\tau_{m,n}\frac{db_{m,n}}{dt} + b_{m,n} = M_{m,n} I_{m,n}$$

m=1 mode wall times

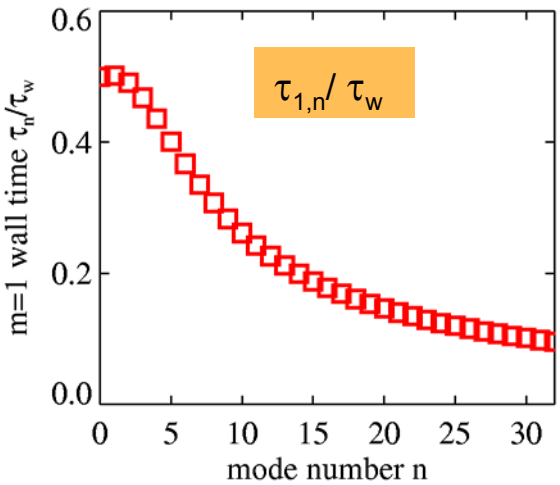

m=1 mode amplitudes

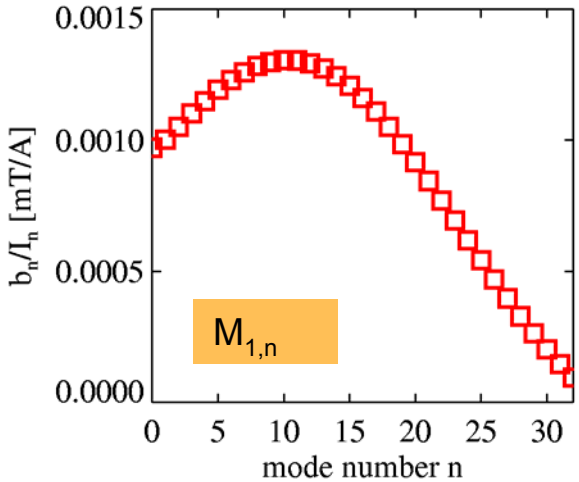

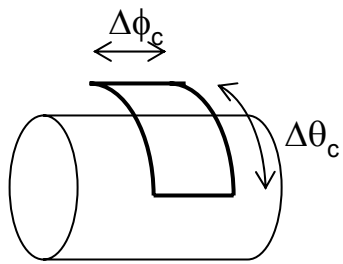

Compare predicted vacuum field with T2R data

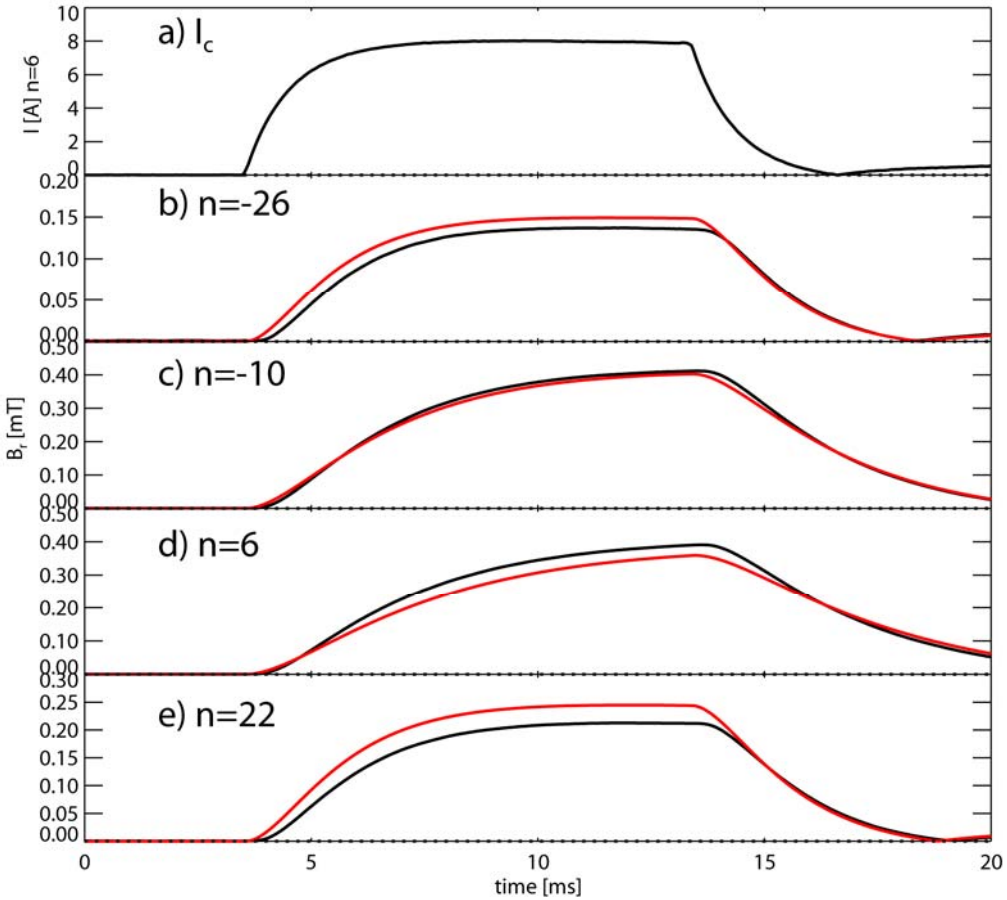

Exp. vacuum field compared to cylindrical model calculation

Radial field mode amplitudes for n=6 coil current harmonic and 4x16 coils

Black: measurement

Red: cylindrical model calc.

T2R data agree well with model values for mode wall times $\tau_{m,n}$ and coil field coefficients $M_{m,n}$

$$\tau_{m,n}\frac{db_{m,n}}{dt}+b_{m,n}=M_{m,n}I_{m,n}$$

Plasma response to saddle coil field harmonics - cylindrical model

Total radial field harmonic at wall $b_{m,n}$ including plasma RWM response to external coil field:

Resistive wall mode growth rate: $\gamma_{m,n}$

Long wall time constant: $\tau_w = \mu_0 \sigma r_w \delta_w$

Mode wall time: $\tau_{m,n}$

Coil field mode coeff.: $M_{m,n}=b_{m,n} / I_{m,n}$

$$\tau_{m,n}\frac{db_{m,n}}{dt} - \gamma_{m,n}\tau_{m,n}b_{m,n} = M_{m,n}I_{m,n}$$

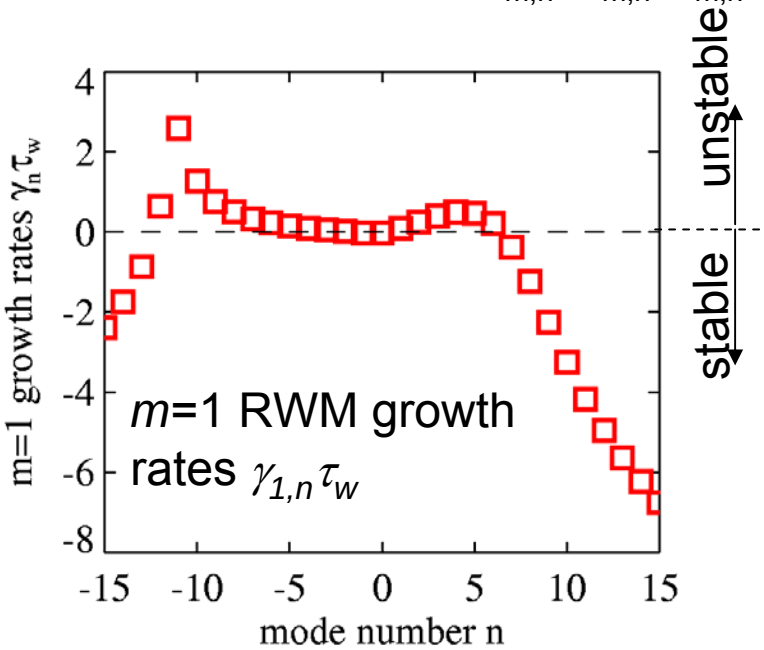

For EXTRAP T2R reversed-field pinch:

- unstable RWMs mainly due to non-resonant, current driven, ideal MHD m=1 kink modes
- ***finite range of unstable m=1 with different toroidal mode number n***
- ***range increases with aspect ratio***
- ***16 unstable modes***

Per Brunsell, RWM control in T2R

Compare model calculated plasma response with measurements

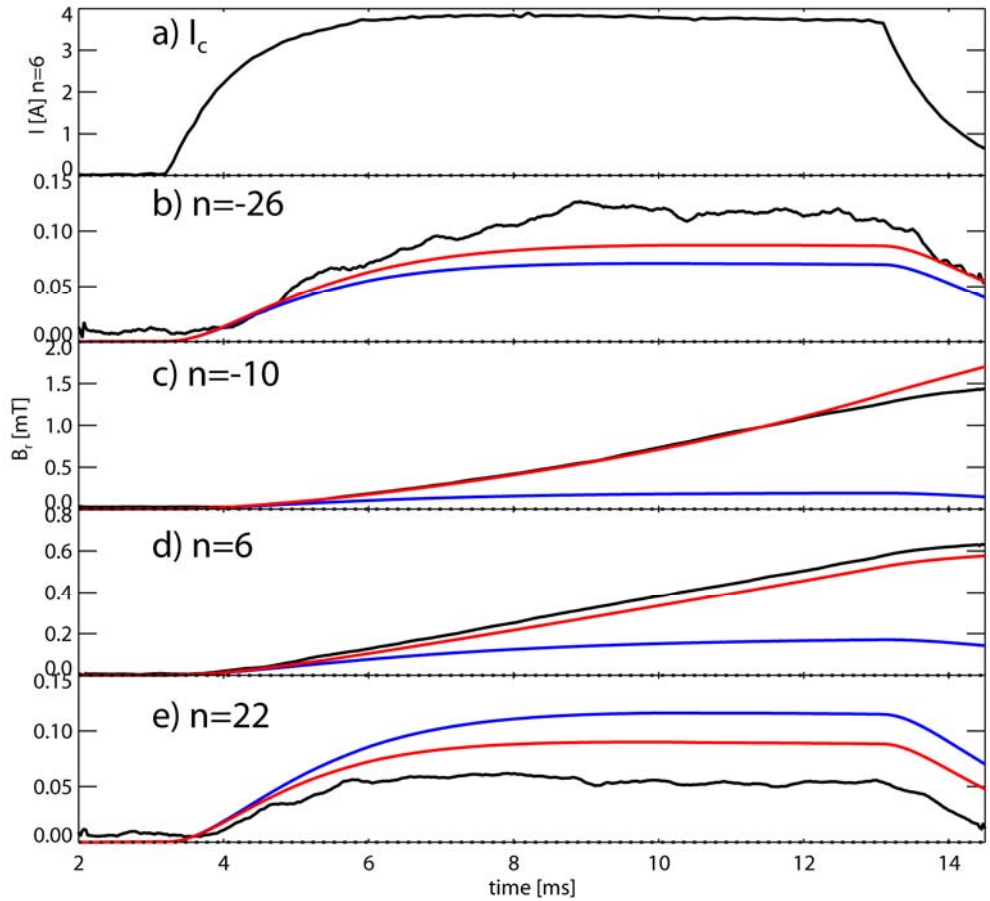

$$\tau_{m,n}\frac{db_{m,n}}{dt} - \gamma_{m,n}\tau_{m,n}b_{m,n} = M_{m,n}I_{m,n}$$

Exp. plasma response to coil field compared with cylindrical model calculation

Radial field mode amplitudes for n=6 coil current harmonic

Black: measurement

Red: calculated plasma response using cyl. model

Blue: calculated vacuum field

T2R data agree well with model RWM growth rates $\gamma_{m,n}$

Intelligent shell fb with 4x32 coils (full surface cover)

Modelling of m=1 RWM feedback control with cylindrical linear MHD model for the RFP

Consider (1,n) sensor field harmonics produced by (1,n') coil current harmonic in array with N coils in toroidal direction.

$$b_n^{coil,vac} = I_{n'} M_n, \quad n = n' + qN$$

With plasma:

$$P_n(s) = \frac{b_n^{coil,pla}}{I_{n'}} = \frac{M_n}{\tau_n (s - \gamma_n)}$$

Mode control with feedback gains G_n:

(G_n = coil current harmonic/ sensor field harmonic)

$$b_n + P_n(s) \sum_q G_{n+qN} b_{n+qN} = b_n^{pert}$$

Modes n=n'+qN are linearly coupled through feedback coils. With no coupled unstable modes, the critical gain for stability is obtained from:

$$1 + G_n P_n(s_n) = 0$$

For stabilization:

$$\mathrm{Re}\{s_n\} < 0, \quad G_n M_n > \tau_n \gamma_n$$

Model prediction of minimum feedback gain for m=1 mode stabilization

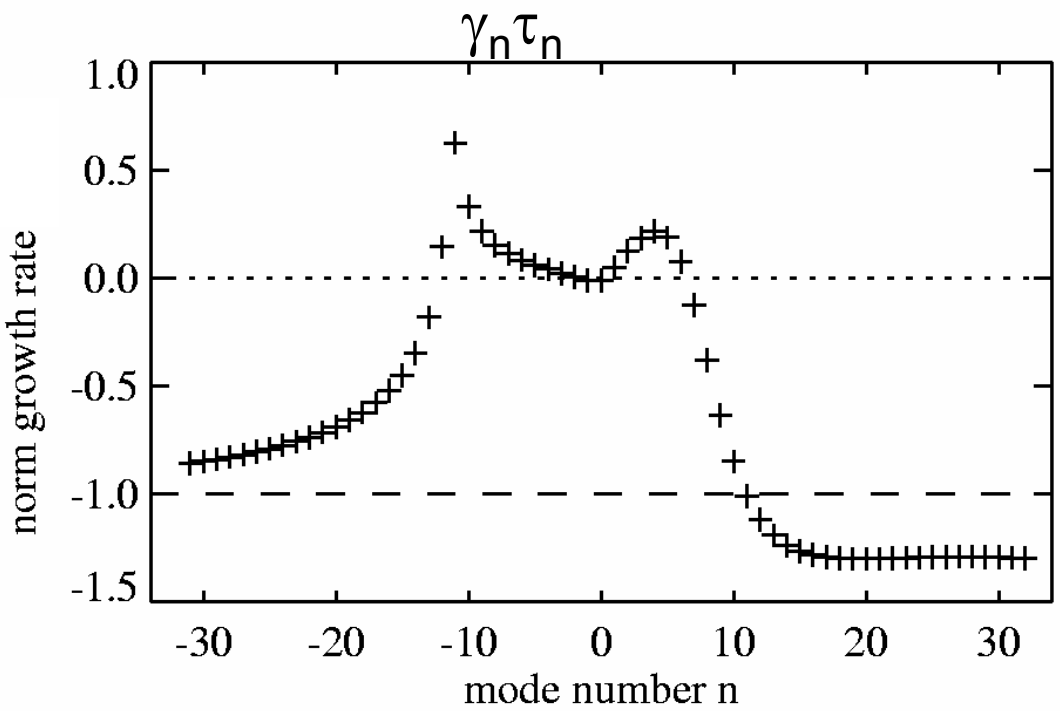

Loop gain for b-radial sensor: $G=b_r^{coil} / b_r^{set}$

b_r^{coil} = b-radial sensor field from coil for b_r^{set}

b_r^{set} = set value of b-radial sensor field

Minimum loop gain G for m=1 mode stabilization:

$G = G_n M_n > \gamma_n \tau_n$

$G_n = I_{coil} / b_{sensor}$

$M_n = b_{sensor,coil} / I_{coil}$ (vac, DC)

γ_n RWM growth rate

τ_n wall time for mode n

The highest gain is obtained for the m=1, n=-11 mode:

$G > 0.7$

Intelligent shell - compare different fb gains

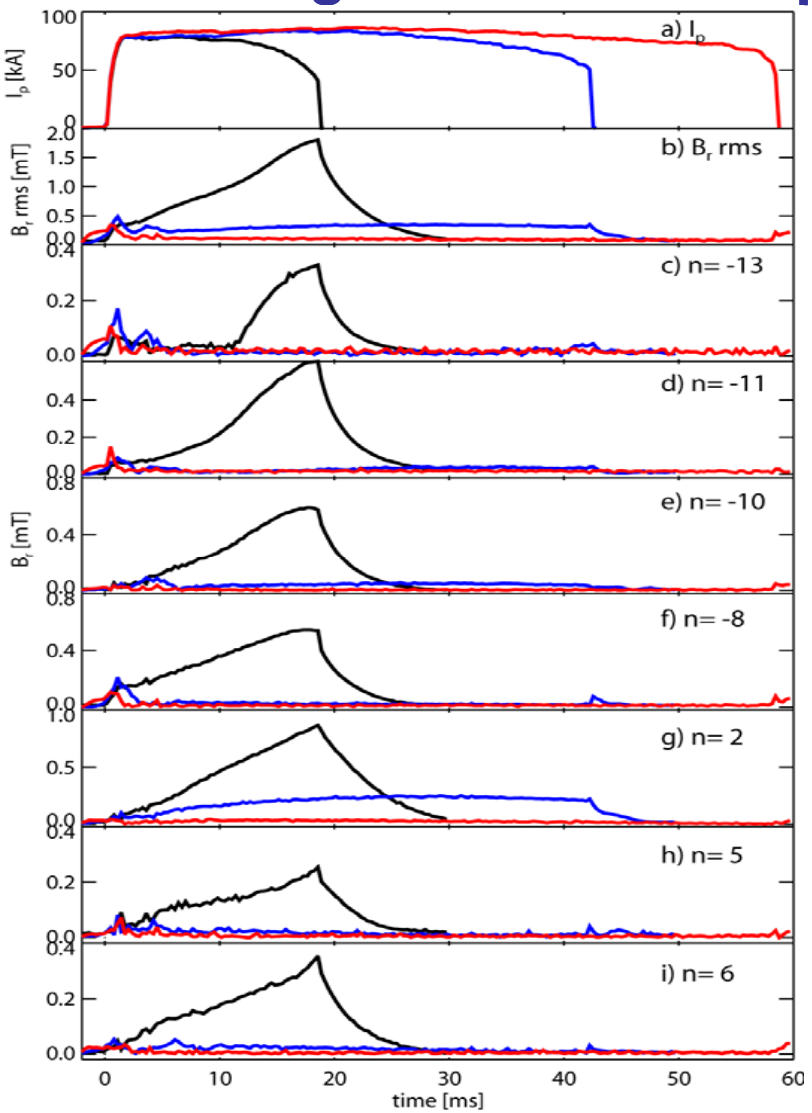

Intelligent shell feedback with 4x32 coils (full surface cover)

black: Ref shot w/o fb

blue: P-control G_P=2.0

red: PID-control G_P=10, G_I=1.3x10^2 s^{-1}, G_D=3.3x10^{-3} s

Without feedback, n=+2 mode has high amplitude, being driven by external field error, mode is not fully suppressed with G=2.

With high fb gain (G=10) and PID-control:

- suppression of n=+2 mode is achived
- discharge prolonged to 10 wall times (60 ms)
- m=1 rms value is suppressed indicating that all unstable m=1 RWMs are suppressed

Feedback gains higher than the model prediction is required for suppression of high amplitude mode driven by field error.

Per Brunsell, RWM control in T2R

Intelligent shell fb - plasma parameters

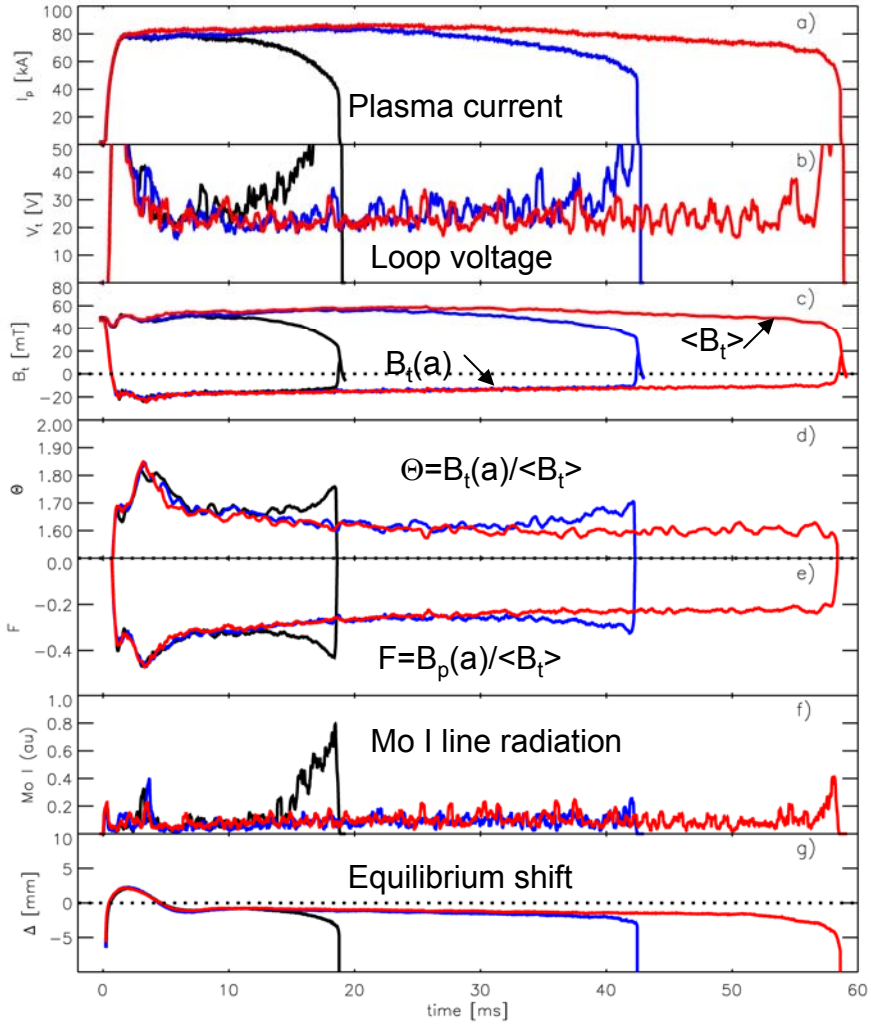

Intelligent shell feedback with 4x32 coils (full surface cover)

black: Ref shot w/o fb

blue: P-control $G_P=2.0$

red: PID-control $G_P=10$, $G_I=1.3\times10^{2}\ s^{-1}$, $G_D=3.3\times10^{-3}\ s$

Loop voltage and Mo impurity influx increases with mode growth toward end of discharge in the case without feedback

With full feedback control loop voltage and impurity influx remain constant

Intelligent shell fb - TMs

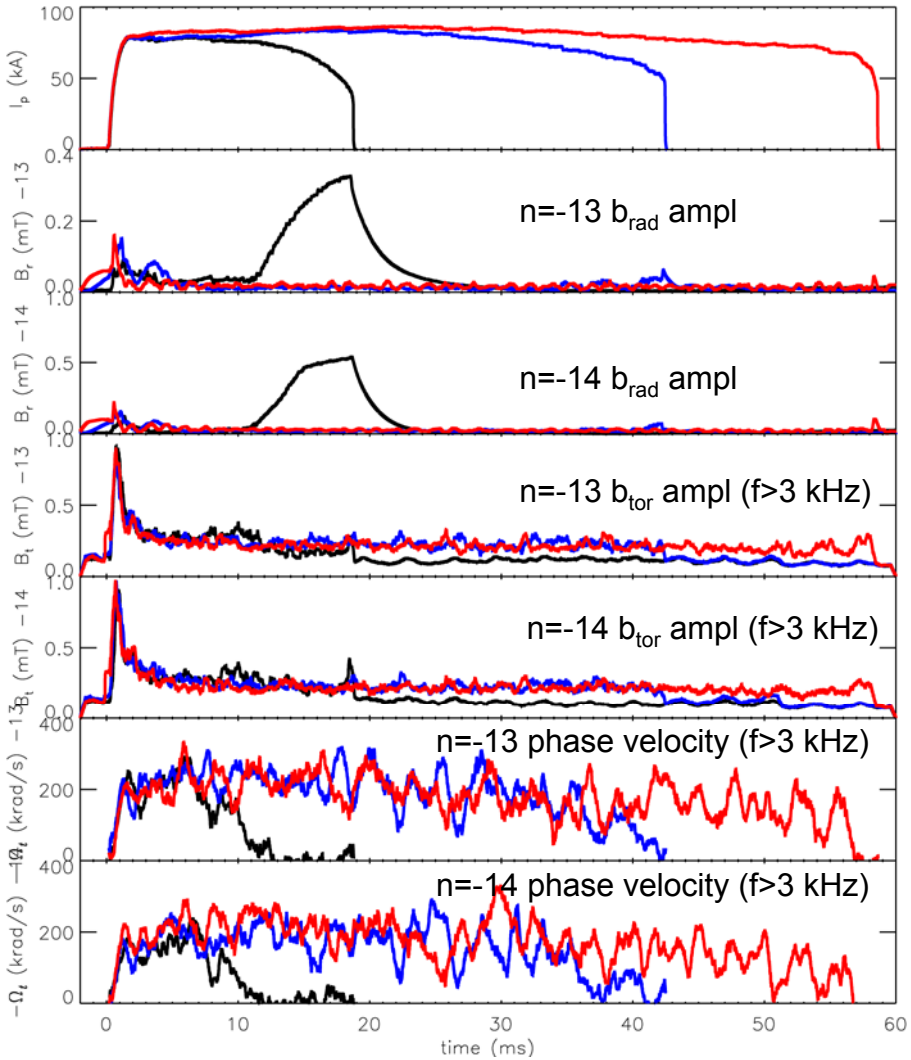

Intelligent shell feedback with 4x32 coils (full surface cover)

Time evolution of two centrally resonant TMs m=1, n=-13 and m=1, n=-14

black: Ref shot w/o fb

blue: P-control G_P=2.0

red: PID-control G_P=10, G_I=1.3x10^2 s^{-1}, G_D=3.3x10^{-3} s

Typical TM phase velocity is about 200 krad/s, corresponding to a toroidal rotation velocity of the order of 20 km/s, similar to the ion toroidal rotation velocity.

Slowing down of TM rotation is delayed further with higher fb gain

Toroidal side band coupling with 4x16 coil feedback

Toroidal side band harmonics with 4x16 coils

Example: m=1, n=+6 coil current

Array with 4x16 coils

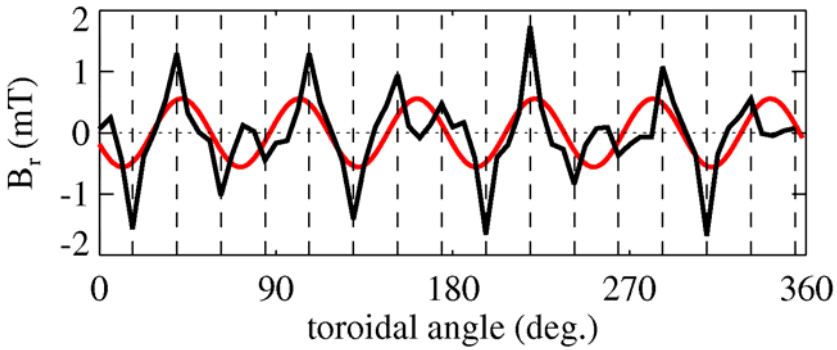

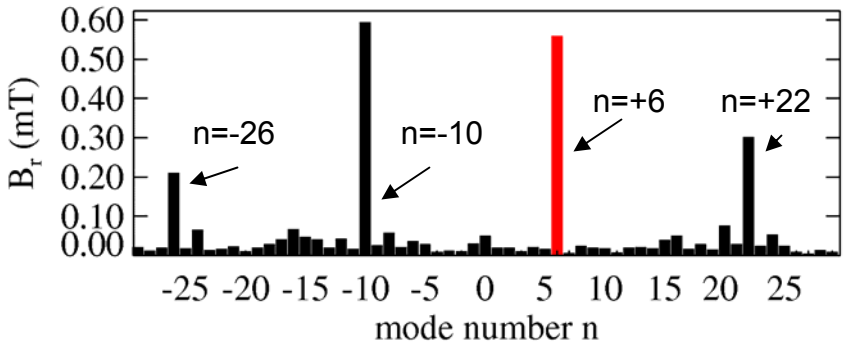

Array with 4x32 coils

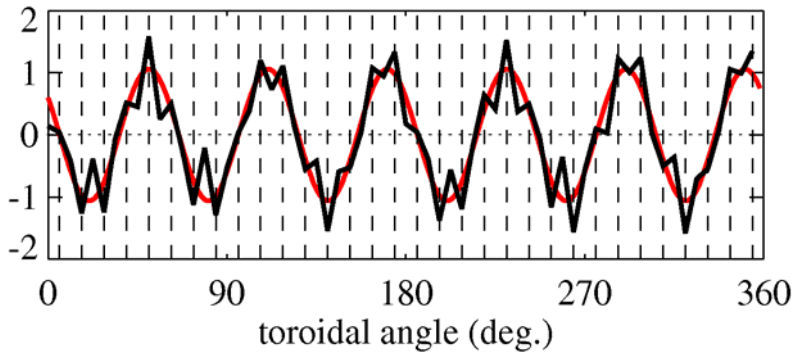

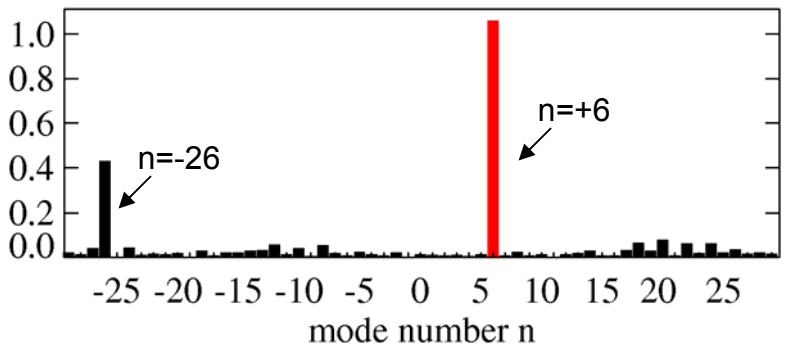

Side band harmonics: $\Delta n = 16$

- ***With feedback control, linear coupling of side band modes***
- ***pairs of coupled unstable RWMs***

Side band harmonics: $\Delta n = 32$

- Mode amplitudes two times higher
- ***No coupled unstable RWMs***

Experimental observation of toroidal side band coupling with intelligent shell feedback

The toroidal side band effect with:

M_c = 4, N_c=16, Δn_c = 16

Compare the m=1,*n* = -10 mode and the coupled m=1, *n* =6 mode.

- The *n*=-10 mode is dominant, so the sideband effect of the *n* = -10 mode on the *n* = 6 mode dominates.
- The end result is a partial suppression of the *n* = -10 mode and faster growth of the *n*=6 mode.
- Both modes have the same amplitude with fb

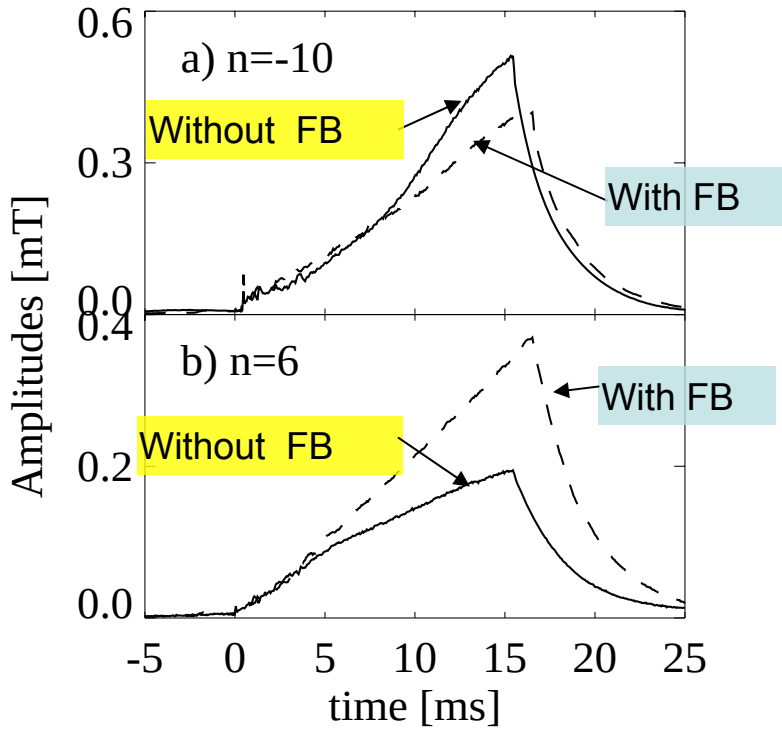

Toroidally coupled side band modes - spatial variation of radial field and mode spectrum

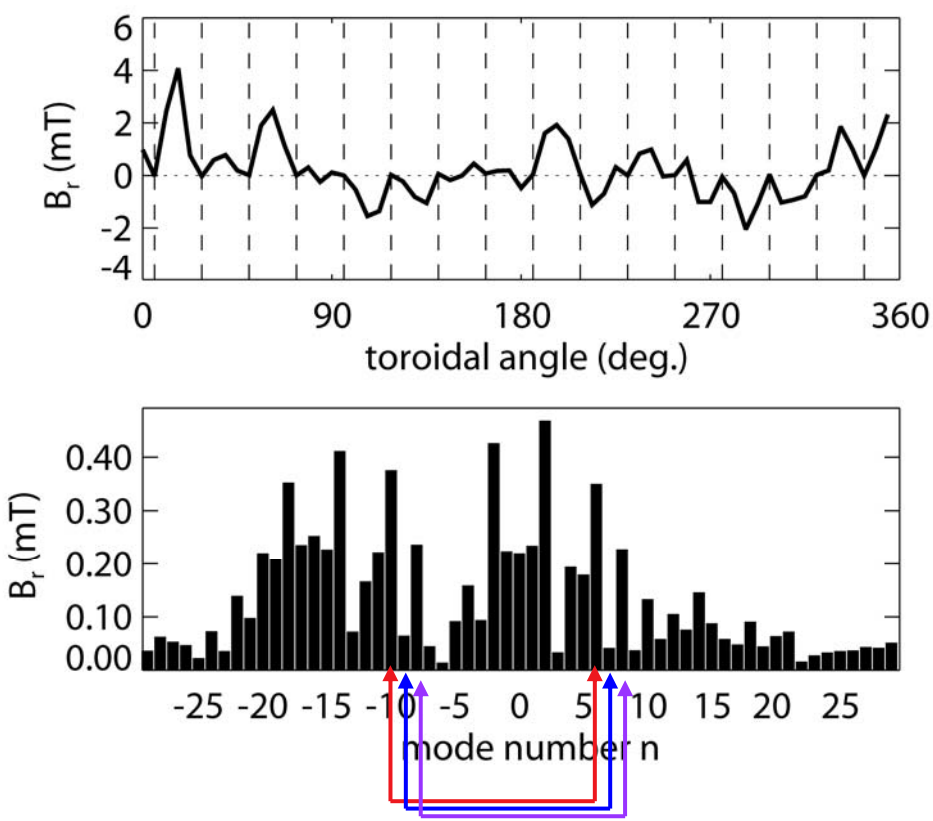

Coupled modes have toroidal mode number difference $\Delta n=16$

Field is suppressed at active coil positions (vertical lines)

Coupled modes are not suppressed – their sum at coil positions is zero due to modes having similar amplitude and π phase difference

Examples in figure:

Modes n=-10, +6

Modes n=-9, +7

Modes n=-8,+8

Modelling of feedback control of two unstable linearly coupled m=1 modes n, n'

Two coupled equations: $$b_n + P_n(s)\left(G_n b_n + G_{n'} b_{n'}\right) = b_n^{pert}$$

Coil-sensor transfer function: $$P_n(s) = \frac{b_n^{coil,pla}}{I_{n'}} = \frac{M_n}{\tau_n\left(s - \gamma_n\right)}$$

Intermediate growth rate: $$\gamma_{n,n'} = \left(g_n \gamma_{n'} + g_{n'} \gamma_n\right) / \left(g_n + g_{n'}\right), \quad g_j = G_j M_j / \tau_j$$

Assume exponentially growing perturbation for mode n only: $$b_n^{pert}(t) = b_n^{pert}\left(\exp\left(\gamma_n t\right) - 1\right), \quad b_{n'}^{pert}(t) = 0$$

At high feedback gains, both modes grow at the intermediate growth rate: $$\frac{b_n}{b_n^{pert}} \approx \frac{g_{n'}}{g_n + g_{n'}} \frac{\gamma_n}{s\left(s - \gamma_{n,n'}\right)}$$

With intelligent shell feedback, the gains for both modes are equal, and *the modes have equal amplitudes with π phase diff.*: $$\frac{b_{n'}}{b_n} \approx -\frac{G_n}{G_{n'}} = -1$$

Sum of modes at coil positions is suppressed, but each coupled mode grows with the same intermediate growth rate $\gamma_{n,n'}$

Poloidal side band coupling with 2x32 coil feedback

Poloidal side band harmonics with 2x32 coils

- Experiments with N_c = 32 but with only 2 coils in the poloidal direction, M_c = 2 (equivalent to sine component only).
- Poloidal sideband effect is important because the m = -1 and m = 1 modes with same n are coupled.
- A control harmonic for mode numbers (m, n) = (1, n) has a side band (-1,n). Using only m=+1 the sideband is (1,-n)
- The amplitudes of the coupled modes are equal.

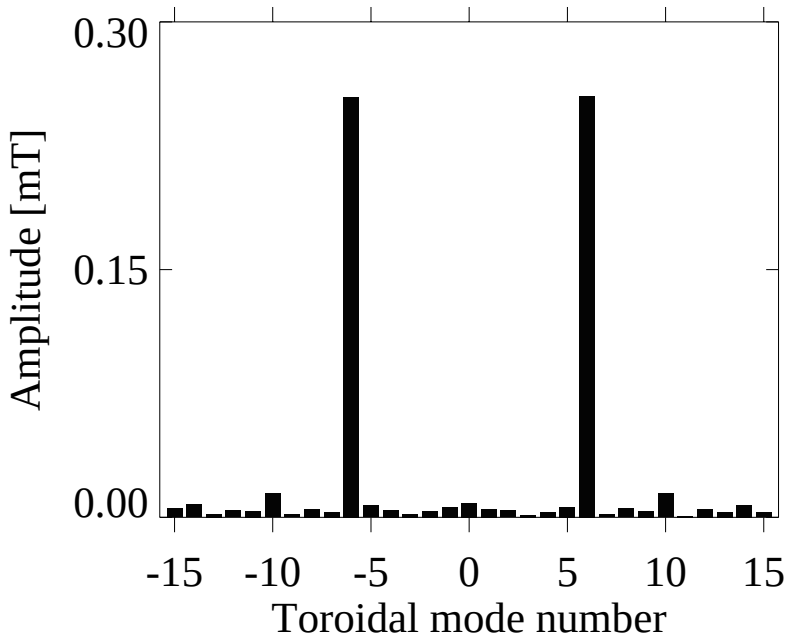

The measured vacuum |m|=1 mode spectrum for a pre-programmed n = 6 perturbation for the active coil configuration with M_c=2 and N_c=32.

Experimental observation of poloidal side band coupling with intelligent shell feedback

The side band effect with:

- M_c = 2, N_c=32, Δm_c = 2
- m=+1 and m = -1 modes are coupled

- Compare the n = 6 mode and the coupled n = -6 mode.

- The n= 6 mode is dominant, so the sideband effect of the n = 6 mode on the n = -6 mode dominates.

- The end result is a partial suppression of the n = 6 mode and faster growth of the n = -6 mode and they have the same amplitude.

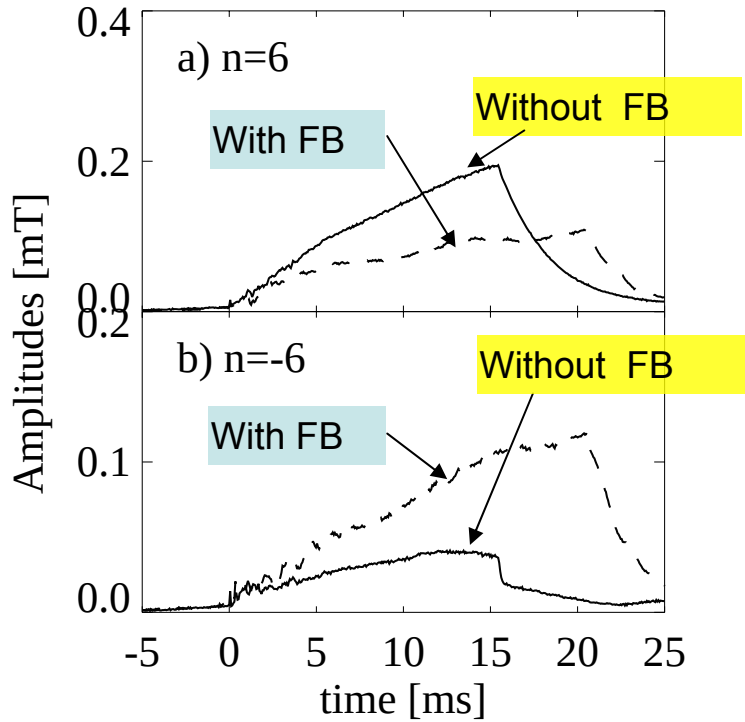

The time dependence of mode harmonic amplitudes.

(a) m=1, n=6. (b) m=1, n=-6.

Test of simplified fake rotating shell feedback

”Fake rotating shell” feedback scheme

[R. Fitzpatrick and T. H. Jensen, Phys. Plasmas 3 (1996) 2641]

Similar idea as intelligent shell: a number of independent active saddle coils acting to suppress wall flux locally

But different from intelligent shell since

• sensor loops are displaced (poloidally or toroidally) relative to control loops causing a phase shift between sensor and control fields

• feedback system acts like a *rotating* secondary shell

The scheme requires that *control and sensor coil dimensions are small compared to the instability wave length*

Preliminary test of a simplified ”fake rotating shell” feedback scheme

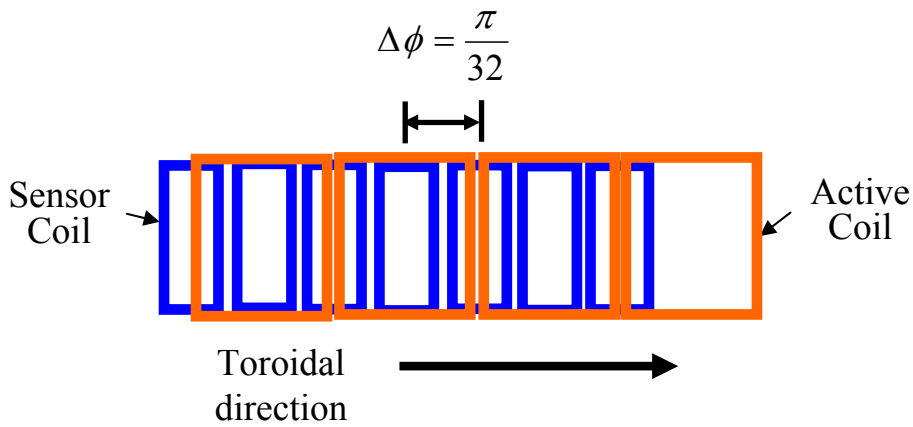

- Use additional sensor coils with c-c separation is $\delta\varphi_s = \pi/32$
- Active coil c-c separation is $\delta\varphi_a = \pi/16$
- Sensor coils are shifted toroidally by $\delta\varphi_s = \pi/32$ relative to active coils
- Phase shift of control field harmonic is $n\delta\varphi_s$ relative to the sensor field harmonic
- Criterion for negative feedback: $n\delta\varphi_s < \pi/2$, or $|n| < 16$

Note that our coils are small compared mode wave lengths only for the low-n modes!

Fake rotating shell - mode time evolution

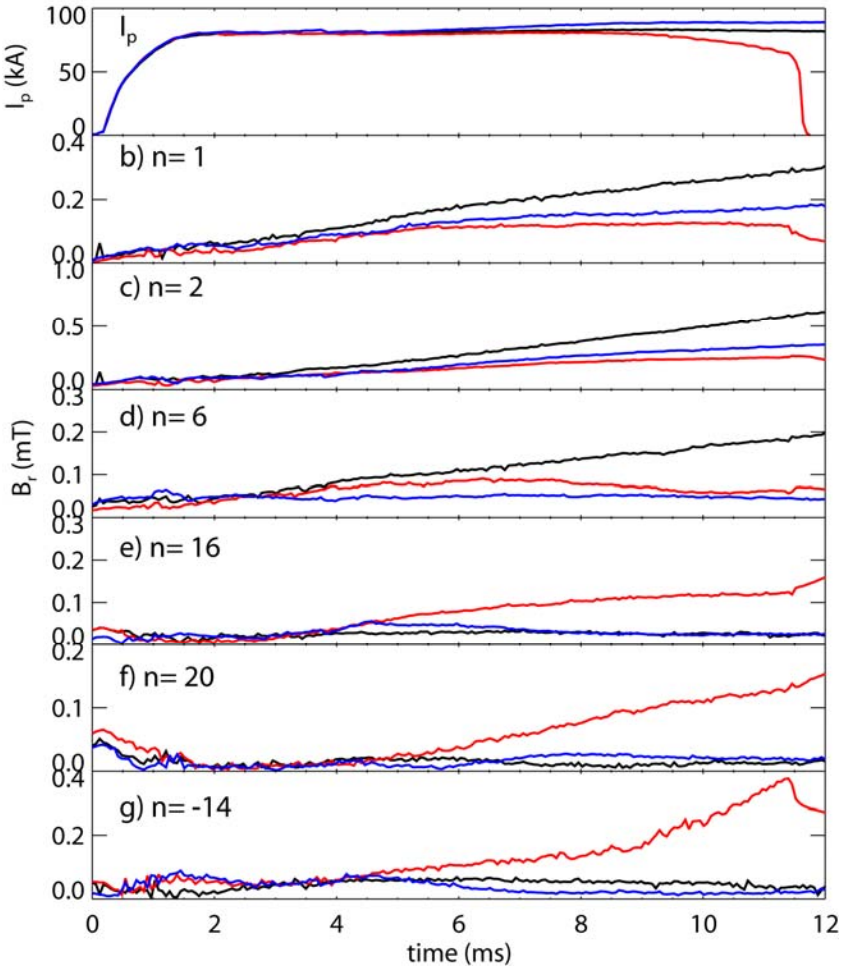

Comparison of fake rotating shell and intelligent shell schemes at low gain G=1.3

Black: shot 18820 ref w/o fb

Blue: shot 18827 intell shell fb

Red: shot 18819 rot fake shell fb

Low-n modes (n=1, 2, 6) suppressed similarly with both schemes

High-n modes (n=16, 20) amplified with rotating fake shell

Tearing mode n=-14 wall locks with rotating fake shell, leading to early discharge termination

Fake rotating shell - mode amplitude spectrum

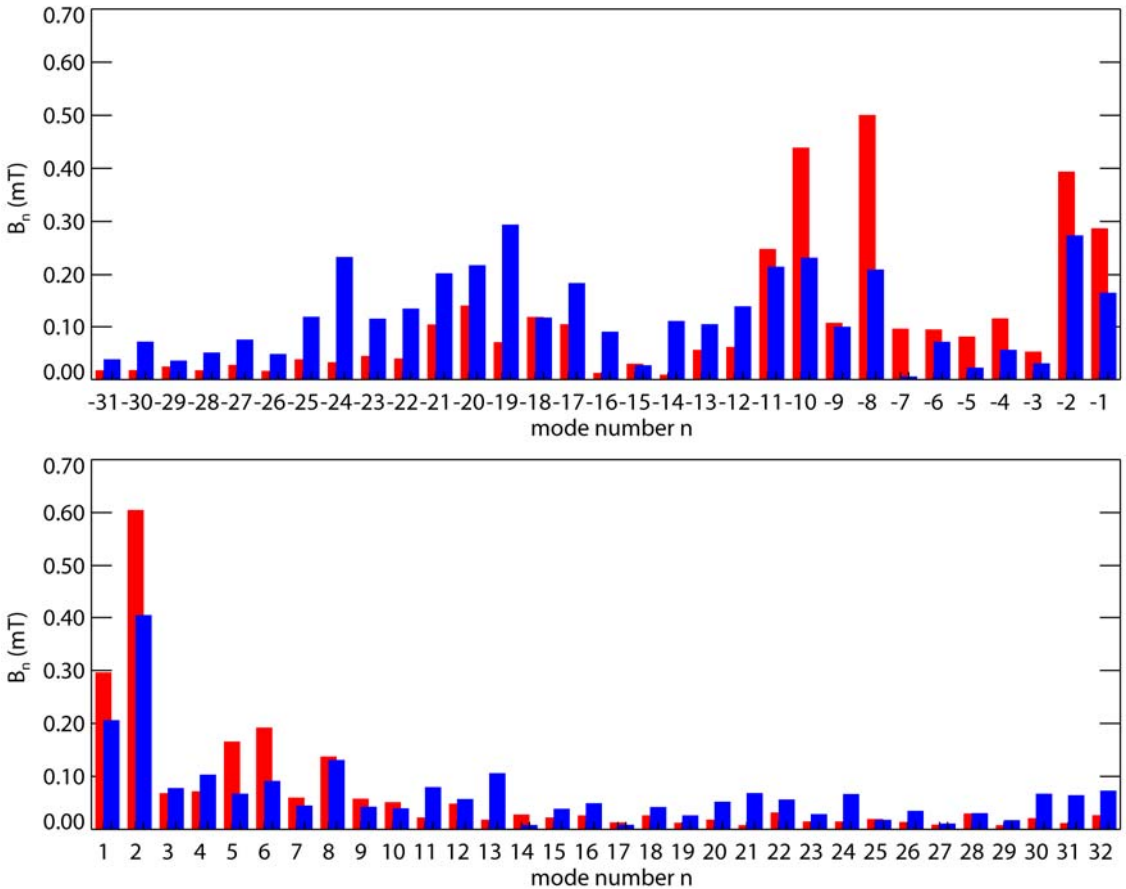

Red: shot 18820 ref w/o fb

Blue: shot 18818 fake rotating shell feedback G=0.65

Negative feedback (stabilizing) expected for modes |n|<16

Positive feedback (destabilizing) expected for modes |n|>16

Results are in qualitative agreement with expectations.

Per Brunsell, RWM control in T2R

Comparison of mode spectrum for fake rotating shell and intelligent shell fb

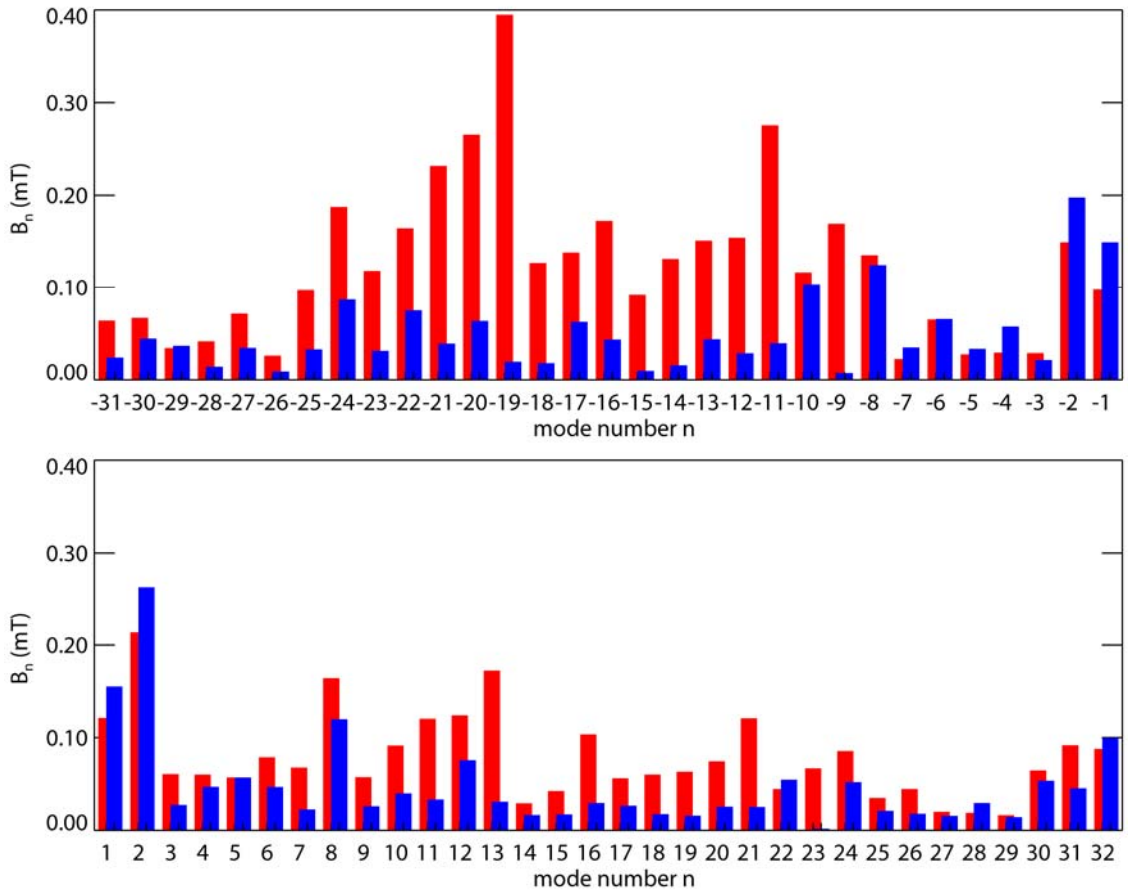

Comparison of feedback schemes using same fb gain (G=1.3)

Red: shot 18819 fake rotating shell feedback

Blue: shot 18827 intelligent shell feedback

Note: Fake rotating shell fb only expected to work for low-n modes

Suppression slightly better with fake rotating shell fb for modes |n|=1,2

Mode rotation with fake rotating shell fb

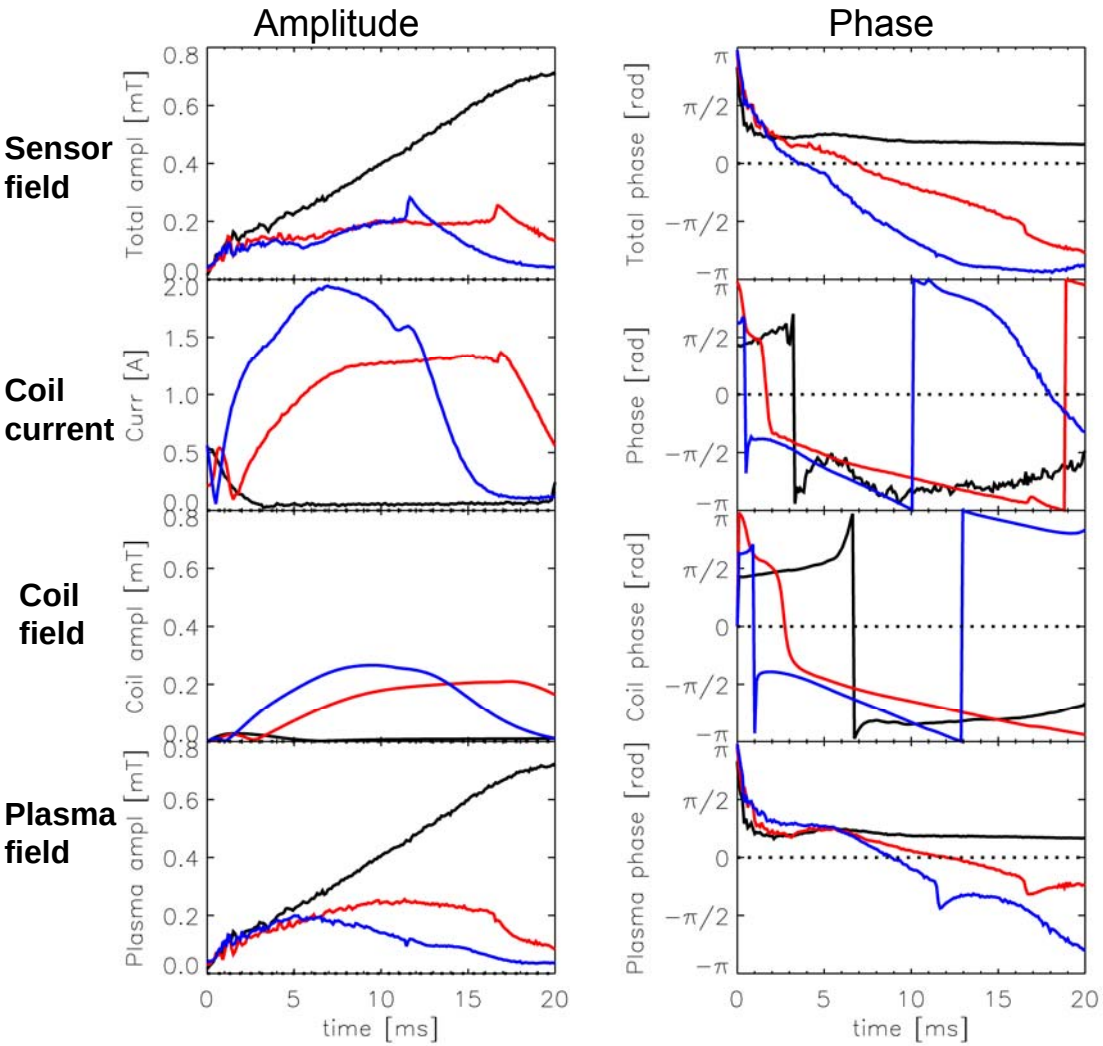

Time evolution of n=-8 mode with fake rotating shell feedback

Black: w/o fb

Red: fb G=0.65

Blue: fb G=1.3

Coil field includes computed wall response. Plasma field is obtained by subtracting coil field from total sensor field

- Coil current and sensor field have phase difference in the range $\pi/4$ - $\pi/2$
- Suppression of plasma field increases with feedback gain
- **fb results in rotation of coil field and plasma field**
- **Rotation speed increases with feedback gain**

Per Brunsell, RWM control in T2R

No mode rotation with intelligent shell fb

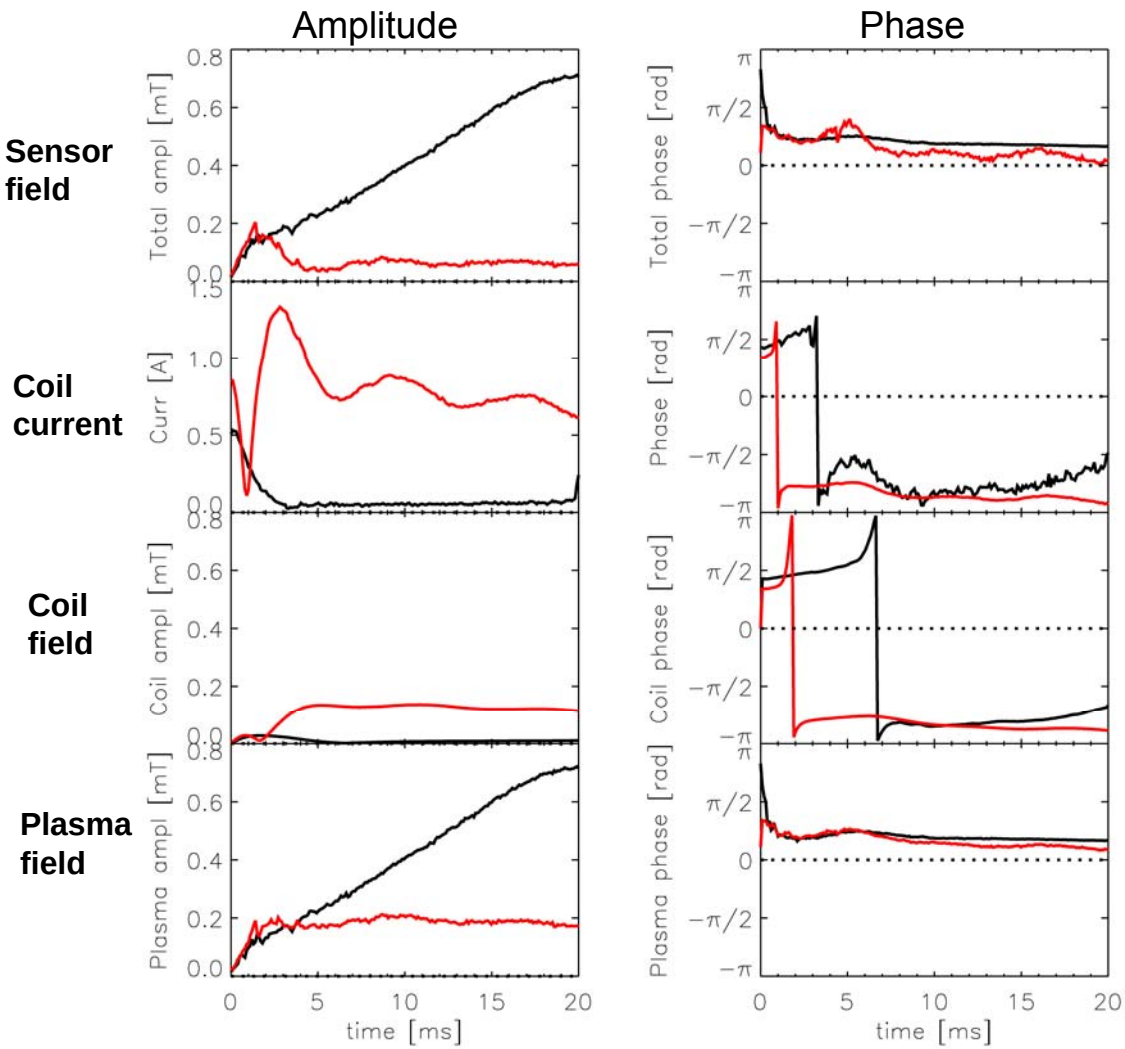

Time evolution of n=-8 mode with intelligent shell fb

Black: w/o fb

Red: fb G=1.3

- Coil current and sensor field have phase difference π
- No rotation is induced

Per Brunsell, RWM control in T2R

Mode control feedback with complex fb gain

”Mode control” feedback scheme

[R. Paccagnella, D. Gregoratto, and A. Bondeson, Nucl. Fusion 42 (2002) 1102]

- Arrays of sensor and active coils are used
- Digital controller is used to compute real-time FFT in order to resolve the spatial Fourier mode spectrum (m,n)
- Controller uses individual feedback gain for each Fourier harmonic (real or complex)

Mode control with complex fb gain

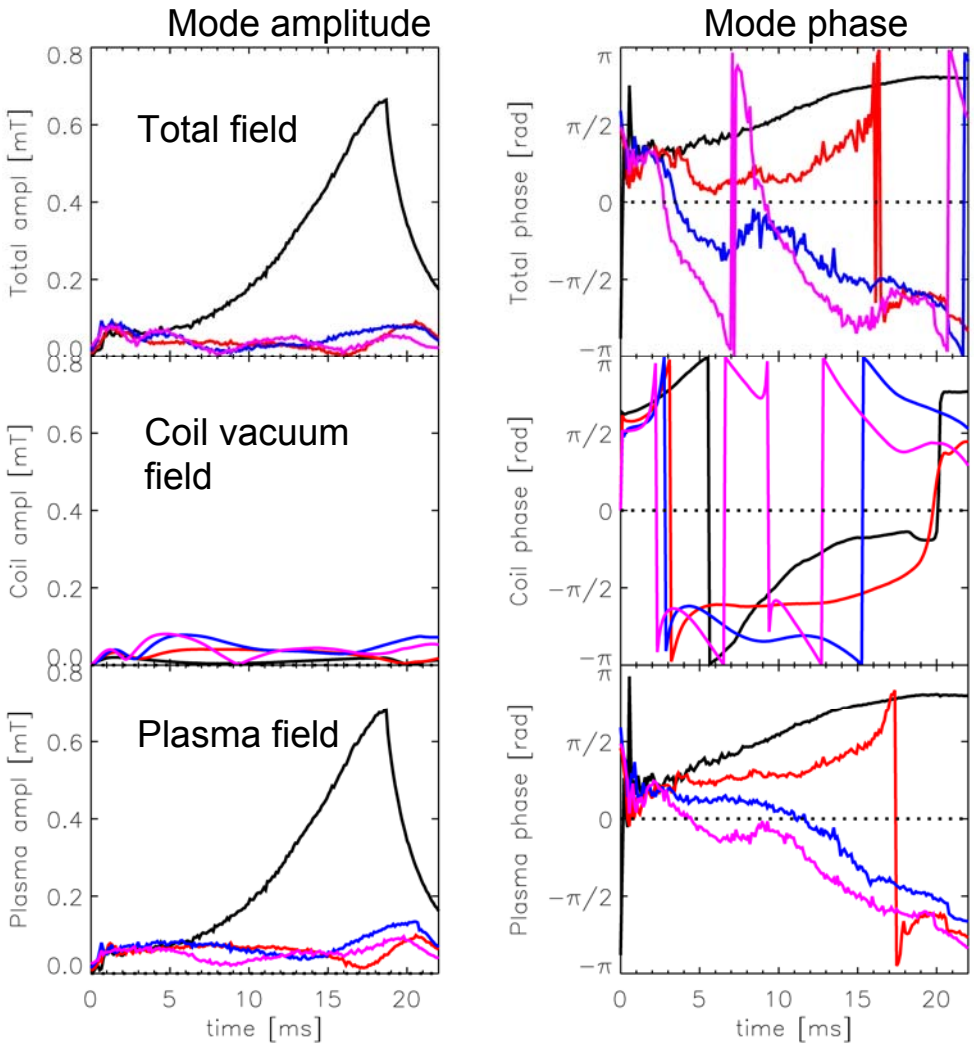

Mode control of n=-11 with complex gain

G=|G|exp(iα)

Vary |G| for α=π/6

Black: w/o fb

Red: fb |G|=0.65

Blue: fb |G|=1.3

Magenta: fb |G|=2.0

- Complex gain results in rotation of plasma field
- Rotation speed increases with magnitude of feedback gain
- Plasma and coil field rotation similar for lower gains, but coil field rotates faster than plasma field for highest gain value

Comparison of mode control with real and complex fb gains

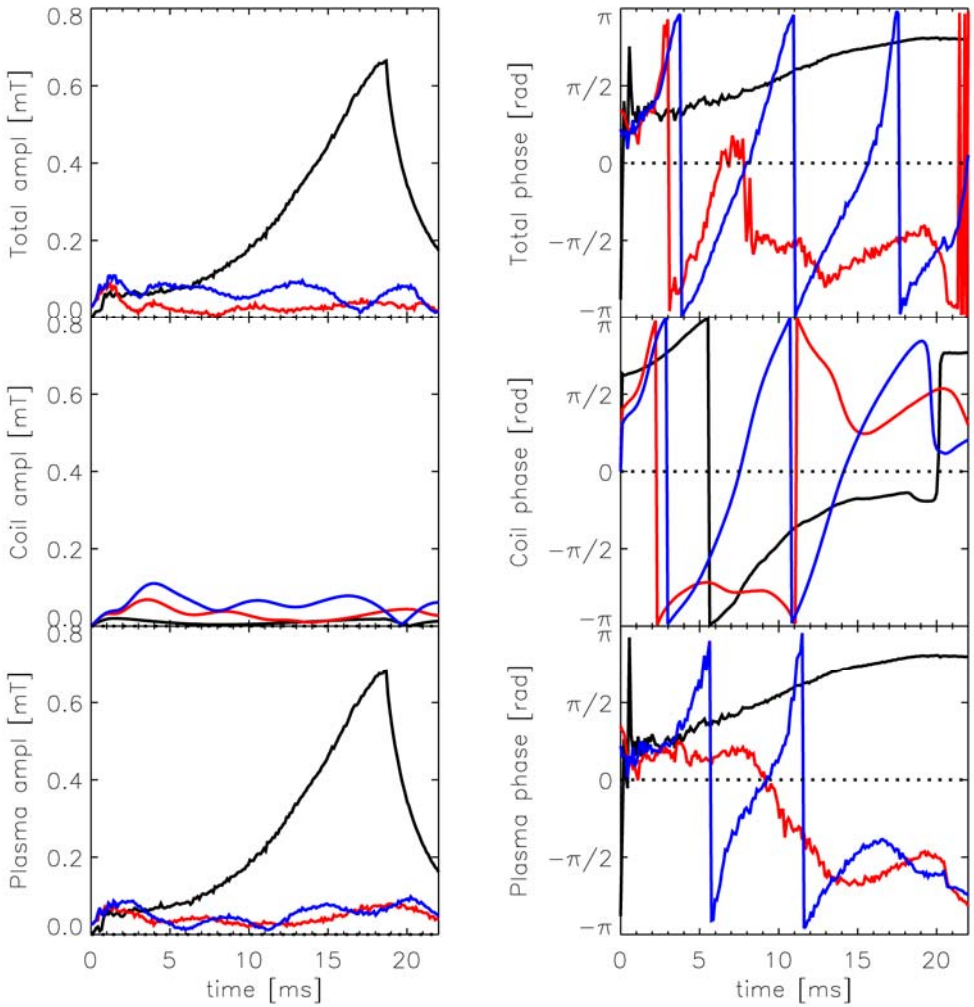

Control of n=-11 with complex and real gains

G=|G|exp(iα)

Compare α=0 and α=−π/6

Black: w/o fb

Red: fb |G|=2.0, α=0

Blue: fb |G|=2.0, α=−π/6

- Both plasma field and coil field rotates with complex fb gain
- Plasma field similarly suppressed with complex fb gain and real gain
- Coil vacuum field amplitude is somewhat higher with complex gain

Per Brunsell, RWM control in T2R

Conclusions

1. ***Comparison of T2R experiment with cylindrical linear MHD model***
   - Vacuum fields and plasma RWM response in T2R are well described.
2. ***Intelligent shell fb with full 4x32 coil array***
   - Higher feedback gain (G=10) than model prediction is required for suppression of high amplitude mode driven by external field error (n=+2).
   - High fb gain and PID control required for suppression of all unstable m=1 RWMs, allowing sustainment of the discharge for 10 wall times (the power supply limit).
3. ***Intelligent shell fb with partial arrays***
   - Toroidal side band mode coupling observed with 4x16 coils. Field is suppressed at coil positions while two coupled modes grow with π phase difference.
   - Poloidal side band mode coupling observed with 2x32 coils.
4. ***Preliminary test of simplified fake rotating shell feedback***
   - Works similar as intelligent shell in suppressing low-n modes, but results also in mode rotation (in contrast to IS). Mode rotation velocity increases with fb gain.
5. ***Mode control feedback***
   - Complex gain results in mode rotation similar as fake rotating shell.